DEVELOPMENT OF BED VARIATION CALCULATION METHOD CONSIDERING NON-EQUILIBRIUM SEDIMENT MOTION AND INTERACTION BETWEEN BED LOAD AND SUSPENSION: APPLICATION TO RIVER MOUTH SANDBAR WITH LARGE-SCALE TOPOGRAPHIC CHANGES DUE TO FLOOD

TAKAHISA GOTOH
Research and Development Initiative, Chuo University, Tokyo, Japan, goto510@tamacc.chuo-u.ac.jp

SHOJI FUKUOKA
Research and Development Initiative, Chuo University, Tokyo, Japan, sfuku@tamacc.chuo-u.ac.jp

ABSTRACT

Large amount of the fine sediments around river mouth are transported in states of suspensions during a flood. The suspended sediment entrainments are characterized by interactions between bed load motions and suspensions of the sediments. In general, the suspended sediment entrainments which was the boundary conditions at the bottom of the advection-diffusion equation of suspended sediment concentrations were estimated by applying equilibrium conditions of sediment motions. In this study, the quasi-three dimensional flow and bed variation analysis method considering the non-equilibrium flows and sediment motions with large amount of suspended sediments was developed. And the interactions between bed load motions and suspensions was also taken into account the bed variation analysis method. The developed analysis method was applied to the 2011flood in the Aganogawa River with large-scale topographical changes in the river mouth sandbar. The calculation results elucidated the enlargements processes of opening widths in the river mouth sandbar and sediment depositions to the downstream toward sea due to the flood.

Keywords: *sediment entrainment, suspended load, non-equilibrium sediment motions, quasi-three dimensional flow and bed variation analysis, river mouth sandbar*

1. INTRODUCTION

The bed materials around the mouth of the lowland river are composed of fine sands, and most of the fine sediments are transported in states of suspensions during floods. The suspended sediment entrainments are caused by translating from bed load to suspensions in high shear stresses of the flow. Therefore, the sediment entrainments are characterized by the interactions between bed load motions and suspended sediments motions.

In general, the bed variation analysis of sandy rivers has been conducted by applying the equilibrium bed load equations and the two-dimensional or three-dimensional advection-diffusion equation for suspended sediments. In the advection-diffusion equation of suspended sediment concentrations, the suspended sediment entrainments which were the boundary conditions of the equation at the bottom have been evaluated by the bed load concentration near the bed in equilibrium conditions (van Rijin(1984), Zyserman and Fredsøe(1990), Itakura et al. (1984) etc.). Therefore, the interactions between bed load and suspended sediment motion has not been taken into account in those conventional bed variation analysis method based on the assumption of equilibrium

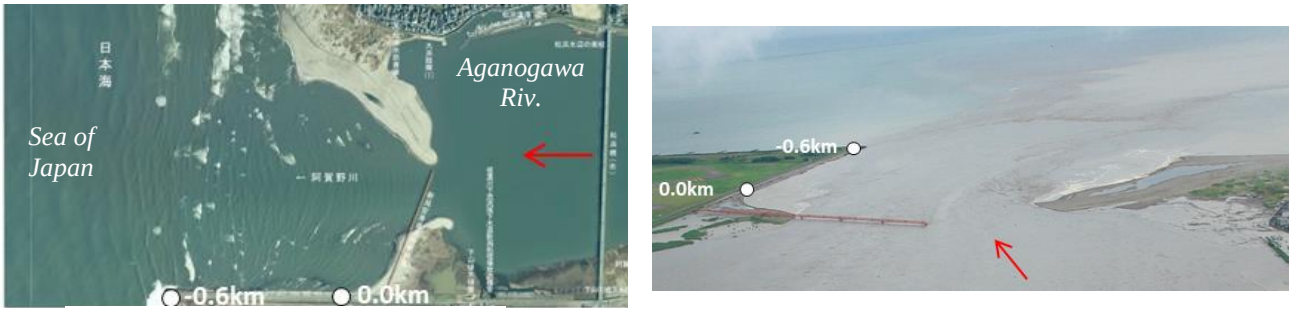

(a) Before the 2011 flood (2010.11.) (b) During 2011 flood (7/30 A.M.8:00)

Figure 1. Aganogawa River mouth sandbar before and during 2011 flood.

conditions. The conventional method has estimated the bed load discharge and suspended sediment entrainments as a function of only friction velocity and could not explained the important mechanism of the non-equilibrium sediment motions for the bed variations.

Nakagawa et. al. (1990) derived the probability density functions per unit time of transitions from saltation motions to suspensions due to turbulence velocity fluctuations assuming the normal distributions. And Bose et. al. (2013) obtained the probability distribution of velocity fluctuations theoretically based on the exponential distributions and investigated the threshold of sediment suspensions from bed load motions. Ota et. al. (2015) applied the Nakagawa(1990)'s transition rates into the three-dimensional flow and two-dimensional bed variation analysis method. However, their calculation method assumed that sand particles were moving in sliding states. The assumption of their calculations was slightly different from the concept of Nakagawa (1990) 's method which estimated the transitions from saltation motions to suspensions. And, verifications of the calculation method were not sufficiently conducted for the sandy rivers where most of fine sediments are transported in suspensions during floods.

In recent years, the three-dimensional and two-phase model of flow and sediment transport have been developed (Chauchat et al. (2017), etc.). The model was able to calculate the bed load motions and suspensions without the assumption of the equilibrium conditions. However, it is difficult to apply the calculation model in the widespread area of rivers having complex bed topographies. The depth integrated model of flood flow and bed variation analysis considering non-equilibrium sediment motion should be constructed to attempt to solve the issues of practical river managements.

Around the river mouth of the Aganogawa River, the large-scale river mouth sandbar composed of fine sands is formed as shown in Figure 1(a). In July 2011, the record breaking largest flood occurred, causing large-scale topographic changes in the river mouth sandbar and enlargements of the opening widths of the river mouth sandbar as shown in Figure 1(b). Tateyama et. al.(2018) developed the quasi-three-dimensional flow and bed variation analysis method considering the effects of the steep slope topography over the sandbar of the Aganogawa River mouth and explained the enlargement processes of the opening widths of the river mouth sandbar. However, their analysis method for bed variations was constructed under the equilibrium conditions of bed load motions and the suspended sediment entrainments, so that the sediments of the eroded river mouth sandbar could not be transported sufficiently downstream toward the sea. Thus the developments of river mouth terrace due deposition of suspended sediments could not be properly explained in their calculation method.

In this study, the analysis method of the quasi-three dimensional flow and bed variation was developed by considering the non-equilibrium flows and sediment motions with large amount of suspended sediments. And the developed method was applied to the 2011flood in the Aganogawa River with large-scale topographical changes in the river mouth.

2. FLOOD FLOW AND BED VARIATION ANALYSIS METHOD CONSIDERING NON-EQUILIBRIUM SEDIMENT MOTIONS WITH LARGE AMOUNT OF SUSPENDED SEDIMENTS

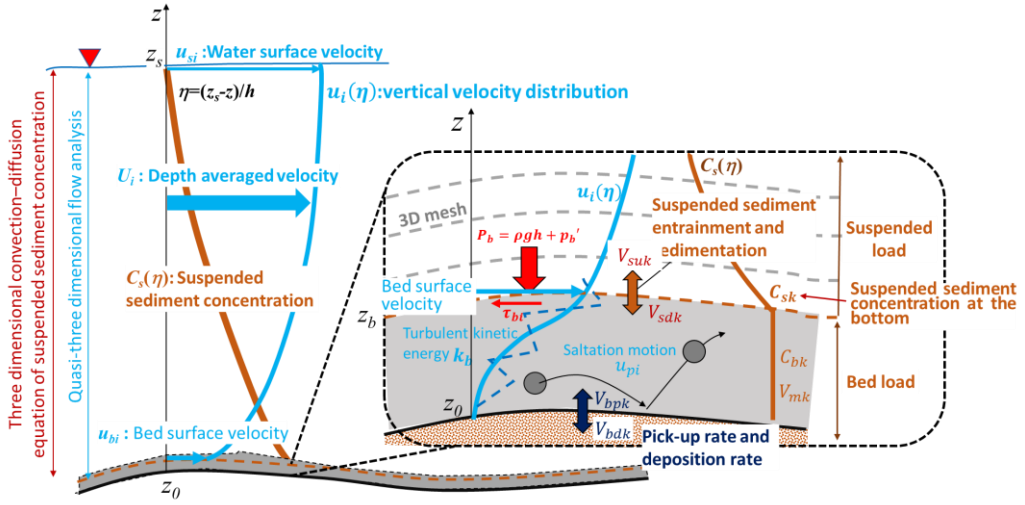

Figure 2. Framework of the calculation method.

Figure 2 shows the framework of the calculation method. The three-dimensional flows and pressure distributions near the beds were calculated by the quasi-three dimensional flow calculation method (Q3D-FEBS method, Takemura & Fukuoka, 2019). The calculation method assumed that the vertical velocity distributions was the third order polynomial in Eq.(1). It was determined by using the mean velocity U_i, the water surface velocity u_{si}, the bed surface velocities u_{bi} and the vertical gradient of velocity at the water surface. Those velocities were calculated by the depth integrated continuity equation in

Eq.(2), the depth integrated horizontal momentum equations in Eq.(3) and the horizontal momentum equation on the water surface and bed surface in Eq.(5) and Eq.(6), where $u_i(\eta)$ is i direction flow velocity at any height, $\Delta u_i = u_{si} - U_i$, $\delta u_i = u_{si} - u_{bi}$, $\eta=(z_s\text{-}z)/h$, U_i is depth averaged flow velocity in i direction, h is water depth, u_{bi} is bed surface velocity, u_{si} is water surface velocity in i direction, z_s is water level, z_b is bed elevation, p'_b is the non-hydrostatic pressure at the bed, ν_t is depth averaged kinematic eddy viscosity coefficient, ν_{ts} and ν_{tb} are kinematic eddy viscosity at water surface and near the bed, respectively. And ρ denotes fluid density, τ_{bi} denotes a shear stresses acting on the river beds and n indicates the Manning's roughness coefficients.

$$u_i(\eta) = U_i + \Delta u_i(12\eta^3 - 12\eta^2 + 1) - \delta u_i(4\eta^3 - 3\eta^2) \tag{1}$$

$$\frac{\partial h}{\partial t} + \frac{\partial U_j h}{\partial x_j} = 0 \tag{2}$$

$$\frac{\partial U_i h}{\partial t} + \frac{\partial U_i U_j h}{\partial x_j} = -gh\frac{\partial z_s}{\partial x_i} - \frac{1}{\rho}\frac{\partial \overline{p'}h}{\partial x_i} - \frac{p'_b}{\rho}\frac{\partial z_b}{\partial x_i} - \frac{\tau_{bi}}{\rho} + \frac{1}{\rho}\frac{\partial hT_{ij}}{\partial x_j} \tag{3}$$

$$\mathrm{T}_{ij} = -\rho\overline{u'_i u'_j} - 2\rho\nu_t S_{ij},\ S_{ij} = \frac{1}{2}\left(\frac{\partial U_i}{\partial x_j} + \frac{\partial U_j}{\partial x_i}\right) \tag{4}$$

$$\frac{\partial u_{si}}{\partial t} + u_{sj}\frac{\partial u_{si}}{\partial x_j} = -g\frac{\partial z_s}{\partial x_i} - \frac{1}{\rho h}\frac{\partial z_s}{\partial x_i}\frac{\partial p'}{\partial \eta}\bigg|_s + \frac{\nu_{ts}}{\rho}\frac{\partial^2 u_{si}}{\partial z^2}\bigg|_s,\quad \frac{\partial^2 u_i}{\partial \eta^2}\bigg|_s = 24\Delta u_i - 6\delta u_i,\ \gamma_{ts} = l_d\sqrt{k_s} \tag{5}$$

$$\frac{\partial u_{bi}}{\partial t} + u_{bj}\frac{\partial u_{bi}}{\partial x_j} = -g\frac{\partial z_s}{\partial x_i} - \frac{1}{\rho}\frac{\partial p'_b}{\partial x_i} - \frac{1}{\rho h}\frac{\partial z_b}{\partial x_i}\frac{\partial p'}{\partial \eta}\bigg|_b + \frac{1}{\rho}\frac{\tau_{bi} - \tau_{0i}}{\delta z_b},\quad \delta z_b = c_{zb}h, c_{zb} = 0.03 \tag{6}$$

$$\frac{\tau_{bi}}{\rho} = -\frac{\upsilon_{tb}}{h}\frac{\partial \overline{u}_i}{\partial \eta}\bigg|_b,\quad \gamma_{tb} = l_d\sqrt{k_b},\qquad l_d = 0.07h$$

$$\frac{\tau_{0i}}{\rho} = c_b^2 u_{bi}|\boldsymbol{u_b}|,\ c_b = \frac{C_0}{1 - 2C_0/\kappa}\sqrt{1 + c_{zb}}, C_0 = \sqrt{\frac{gn^2}{h^{1/3}}} \tag{7}$$

The gradients for vertical directions of the non-hydrostatic pressure at the river bed and water surface in Eq.(5) and in Eq.(6) were calculated by the momentum equations for vertical directions at the beds and water surface in Eq.(8). The non-equilibrium turbulent intensities near the bed are important to estimate the amount of suspended sediments entrainments. The transport equation for the turbulent kinetic energy at the bed k_b in Eq.(11) was calculated in addition to the transport equations for the depth integrated turbulent kinetic energy K in Eq.(9) and the turbulent kinetic energy at the water surface k_s in Eq.(10). The turbulence production term at the bottom in Eq.(11) was expressed by using the bed shear stresses.

$$\frac{1}{\rho h}\frac{\partial p'}{\partial \eta}\bigg|_s = u_{sj}\frac{\partial w_s}{\partial x_j},\qquad \frac{1}{\rho h}\frac{\partial p'}{\partial \eta}\bigg|_b = u_{bj}\frac{\partial w_b}{\partial x_j} \tag{8}$$

$$\frac{\partial K}{\partial t} + U_j\frac{\partial K}{\partial x_j} = P_k - C_d\frac{K^{3/2}}{l_d} + \frac{\upsilon_t}{h\sigma_k}\frac{\partial^2 K}{\partial x^2_j} + \frac{1}{h^2}\frac{\upsilon_{tb}}{\sigma_k}\frac{\partial k_b}{\partial \eta} \tag{9}$$

$$P_k = 0.5h\upsilon_t\left\{\frac{1}{2}\left(\frac{\partial U_i}{\partial x_j} + \frac{\partial U_j}{\partial x_i}\right)^2 - \frac{12}{15h^2}(2\Delta u_i\Delta u_i - 7\delta u_i\Delta u_i + 8\delta u_i\delta u_i)\right\}$$

$$\frac{\partial k_b}{\partial \eta} = 12\,\Delta k - 6\,\delta k, \Delta k = k_s - K, \delta k = k_s - k_b$$

$$k(\eta) = \Delta k(12\eta^3 - 12\eta^2 + 1) + \delta k(-4\eta^3 + 3\eta^2) + K$$

$$\frac{\partial k_s}{\partial t} + u_{sj}\frac{\partial k_s}{\partial x_j} = -C_d\frac{k_s^{3/2}}{l_d} + \frac{\upsilon_{ts}}{\sigma_k}\frac{\partial^2 k_s}{\partial x^2_j} + \frac{1}{h^2}\frac{\upsilon_{ts}}{\sigma_k}\frac{\partial^2 k_s}{\partial \eta^2},\qquad \frac{\partial^2 k_s}{\partial \eta^2} = -24\Delta k + 6\delta k, C_d = 0.08, \sigma_k = 1.0 \tag{10}$$

$$\frac{\partial k_b}{\partial t} + u_{bj}\frac{\partial k_b}{\partial x_j} = P_{kb} - C_d\frac{k_b^{3/2}}{l_d} + \frac{\upsilon_{tb}}{\sigma_k}\frac{\partial^2 k_b}{\partial x^2_j} + \frac{1}{h^2}\frac{\upsilon_{tb}}{\sigma_k}\frac{\partial^2 k_b}{\partial \eta^2},\qquad \frac{\partial^2 k_b}{\partial \eta^2} = 48\Delta k - 12\delta k \tag{11}$$

$$P_{kb} \approx \tau_{bi}\frac{\partial \overline{u}_i}{\partial z}\bigg|_b = \frac{\tau_{bi}^2}{\rho\upsilon_{tb}}$$

The bed variations were calculated by the momentum equations and the continuity equations considering the non-equilibrium motions of bed load and suspended sediments and the interactions between them as follows.

The velocities of the sand particles $\overline{u_{pik}}$ of the bed load in the horizontal direction are evaluated by the saltation analysis (Osada & Fukuoka, 2013) using the momentum equation of a sand particle in Eq.(12) regarding the three dimensional flows calculated by the quasi-three dimensional flow analysis, where A_2 and A_3 are a two-dimensional and three-dimensional shape factor, respectively. ρ_s is sand particle density. k indicates particle numbers and d_k is particle diameter.

The bed load volume per unit width was calculated by the continuity equation of the bed load considering the interactions between bed load motions and suspensions in Eq.(13). Those interactions were estimated by the transition term from bed load to suspensions and sedimentations term from suspensions to bed load motions in the equations. The amount of sedimentation V_{sdk} from suspensions to bed load motions were described as the products of the particle settling velocity w_{sk} and the suspended sediment concentration near the river bed C_{sk} as shown in Eq. (14). The suspended sediment concentration near the river bed C_{sk} was evaluated by the three-dimensional advection-diffusion equations described later. The deposit rate to the river bed per unit time V_{bdk} were also evaluated by the products of the particle settling velocity and the bed load concentration C_{bk}. The bed load concentration C_{bk} was calculated by dividing the bed load volume per unit width by mean saltation heights as shown in Eq. (14). The mean saltation heights were evaluated as three times of each particle size by the saltation analysis. And, the pick-up rate V_{pbk} from the river bed was obtained from Eq.(15) (Osada & Fukuoka, 2013).

The suspended sediment entrainments V_{suk} from the bed load motions were calculated by using the vertical particle velocity w_{pk} near the beds and the bed load concentrations C_{bk} as shown in Eq. (16). The vertical particle velocities w_{pk} were obtained from the vertical momentum equation of a sand particle considering the fluid forces generated by turbulence fluctuations F'_z in addition to the fluid forces by mean flow velocities F_z near the bed (Eq.(17)). The fluid forces due to the turbulence fluctuations F'_z were assumed that the turbulence was isotropic and the velocity fluctuations followed the normal distributions. On the other hand, Bose et.al. (2013) indicated that velocity fluctuations obeyed the Gram-Charlier-based twosided exponential or Laplace distributions. It is necessary to investigate the effects of differences of the probability distribution of turbulent velocity fluctuations in the future.

The suspended sediment transports were calculated by the three-dimensional advection-diffusion equation using those suspended sediment entrainments as the boundary condition at the bed (Eq.(19)). And the temporal changes in the bed elevations was obtained from the continuous equation of the river bed shown in Eq.(20).

$$A_3(\rho_s+\rho C_M)d_k^3\frac{\partial u_{pik}}{\partial t}=\frac{1}{2}\rho C_D A_2 d_k^2(u_{bi}-u_{pi})\left|\boldsymbol{u_b}-\boldsymbol{u_{pk}}\right|-A_3(\rho_s-\rho)g_i d_k^3 \tag{12}$$

$$\overline{u_{pik}}=\frac{1}{T_{sal}}\int_0^{T_{sal}}u_{pik}dt\,,T_{sal}=10$$

$$\frac{\partial V_{mk}}{\partial t}+\frac{\partial q_{bkj}}{\partial x_j}=V_{bpk}-V_{bdk}-V_{suk}+V_{sdk},\qquad q_{bkj}=V_{mk}\overline{u_{pjk}} \tag{13}$$

$$V_{sdk}=C_{sk}w_{sk},\quad V_{bdk}=C_{bk}w_{sk},C_{bk}=V_{mk}/(3d_k) \tag{14}$$

$$V_{bpk}=\varepsilon_p\left(\frac{p_k}{A_2d_k^2}\right)\left(\frac{A_3d_k^3}{T_p}\right) \tag{15}$$

$$V_{spk}=\alpha C_{bk}w_{pk},w_{pk}>0,\alpha=0.2 \tag{16}$$

$$\begin{aligned}A_3(\rho_s+\rho C_M)d_k^3\frac{dw_{pk}}{dt}&=F_z+F'_z-A_3(\rho_s-\rho)g_z d_k^3\\&=\tfrac{1}{2}A_2C_D\rho\mathrm{d}^2\left(w_b+w_b{}'-w_{pk}\right)\left|\boldsymbol{u_b}+\boldsymbol{u'_b}-\boldsymbol{u_{pk}}\right|-A_3(\rho_s-\rho)g_z d_k^3\end{aligned} \tag{17}$$

$$w'_b\approx N(\mu,\sigma),\mu=w_b,\sigma=\sqrt{\overline{w'_{bl}w'_{bl}}},\ \overline{w'_{bl}w'_{bl}}=\overline{v'_{bl}v'_{bl}}=\overline{u'_{bl}u'_{bl}}=2/3k_b \tag{18}$$

$$\begin{aligned}&\frac{\partial C_{sk}\Delta z}{\partial t}+\frac{\partial C_{sk}u\Delta z}{\partial x}+\frac{\partial C_{sk}v\Delta z}{\partial y}+\frac{\partial C_{sk}w\Delta z}{\partial z}\\&=\frac{\partial}{\partial x}\left(\nu_t\Delta z\frac{\partial C_{sk}}{\partial x}\right)+\frac{\partial}{\partial y}\left(\nu_t\Delta z\frac{\partial C_{sk}}{\partial y}\right)+\frac{\partial}{\partial z}\left(\nu_t\Delta z\frac{\partial C_{sk}}{\partial z}\right)+\left(V_{psk}-V_{dsk}\right)\big|_{z_b}\end{aligned} \tag{19}$$

$$\frac{\partial z_b}{\partial t}=-\sum_{k=1}^{kmax}\frac{A_2}{A_3}(V_{bpk}-V_{bdk}) \tag{20}$$

3. OBSERVATIONS AND CALCULATION CONDITION

Figure 3 shows the water level and discharge observation points and the values of the Manning's roughness coefficients. The Manning's roughness coefficients were determined so that the time series of calculated water surface profiles reproduced the observed water surface profiles in the following chapter. The detailed observations of time series of the water surface profiles were conducted between 0.2km to 3.5km points upstream of the river mouth.

The upstream boundary condition of the calculation was the observed water level hydrograph at the Yokogoshi observation station (13.5km point). And the downstream boundary condition was the observed sea level hydrograph at the Niigata Nishi Port observation station.

Figure 4 indicates the observed particle size distributions of bed materials in the objective area. It was found that the bed materials were composed of almost uniform fine sands. Thus, the bed materials in the calculation

was set as a grain size of 0.7mm uniformly at the upstream reaches of 1km point. And the grain size of 0.4mm was given uniformly downstream reaches of 1.0 km point.

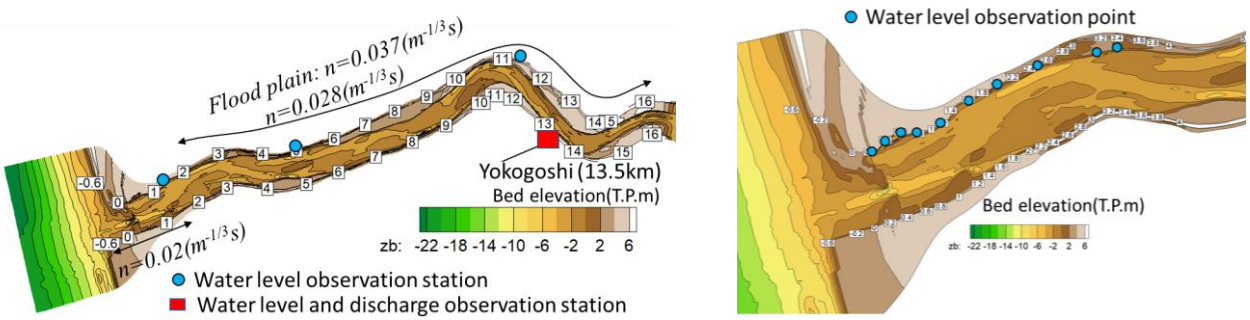

Figure 3. Water level and discharge observation points and the Manning's roughness coefficients.

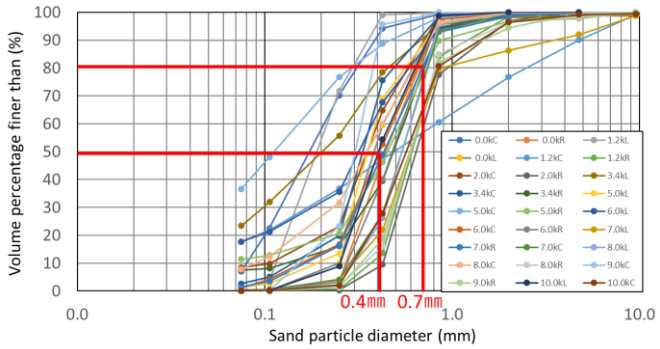

Figure 4. Observed sediment particle sizes and calculation condition.

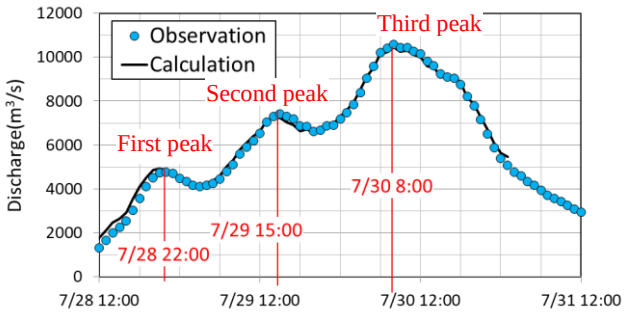

Figure 5. Observed and calculated discharge hydrograph at Yokogoshi(13.5km) observation stations.

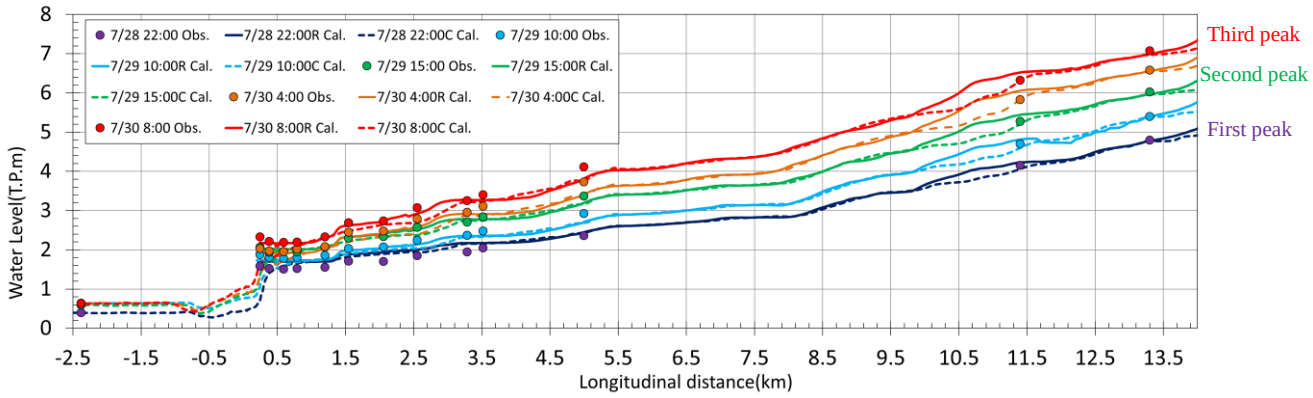

Figure 6. Observed and calculated water surface profiles in the flood rising period.

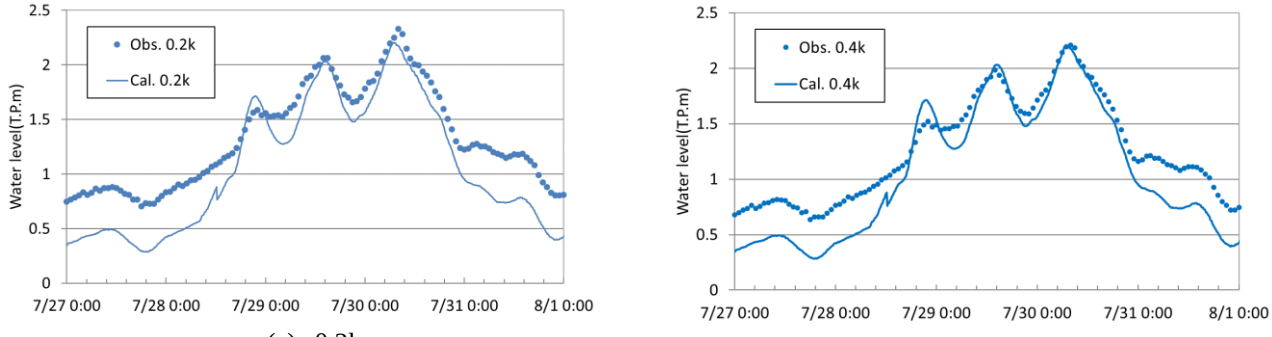

(a) 0.2km (b) 0.4km

Figure 7. Observed and calculated water level hydrographs at 0.2km and 0.4km points.

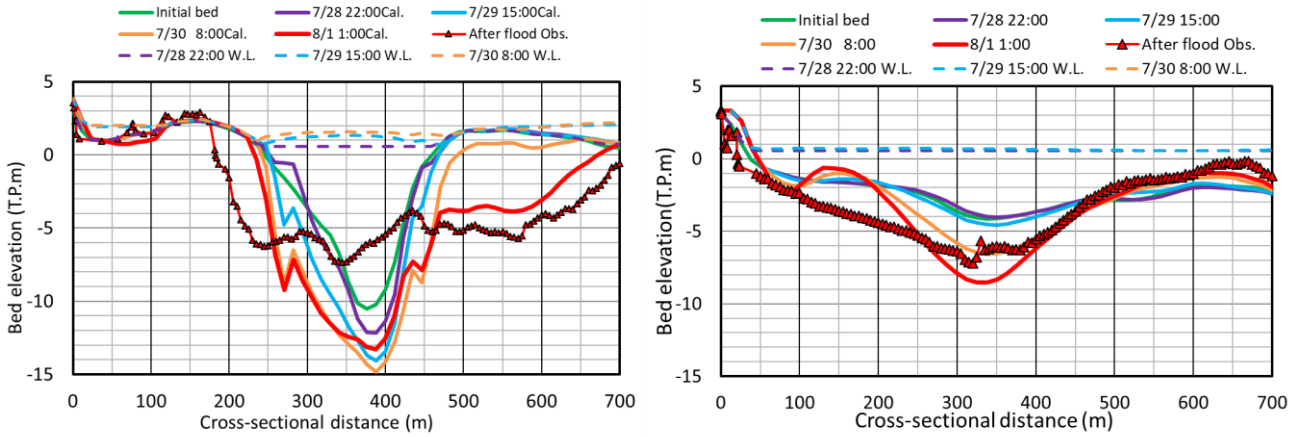

(a) 0.2km (b) -0.45km

Figure 8. Observed and calculated cross-sectional bed profiles of sandbars at the river mouth before and after the flood.

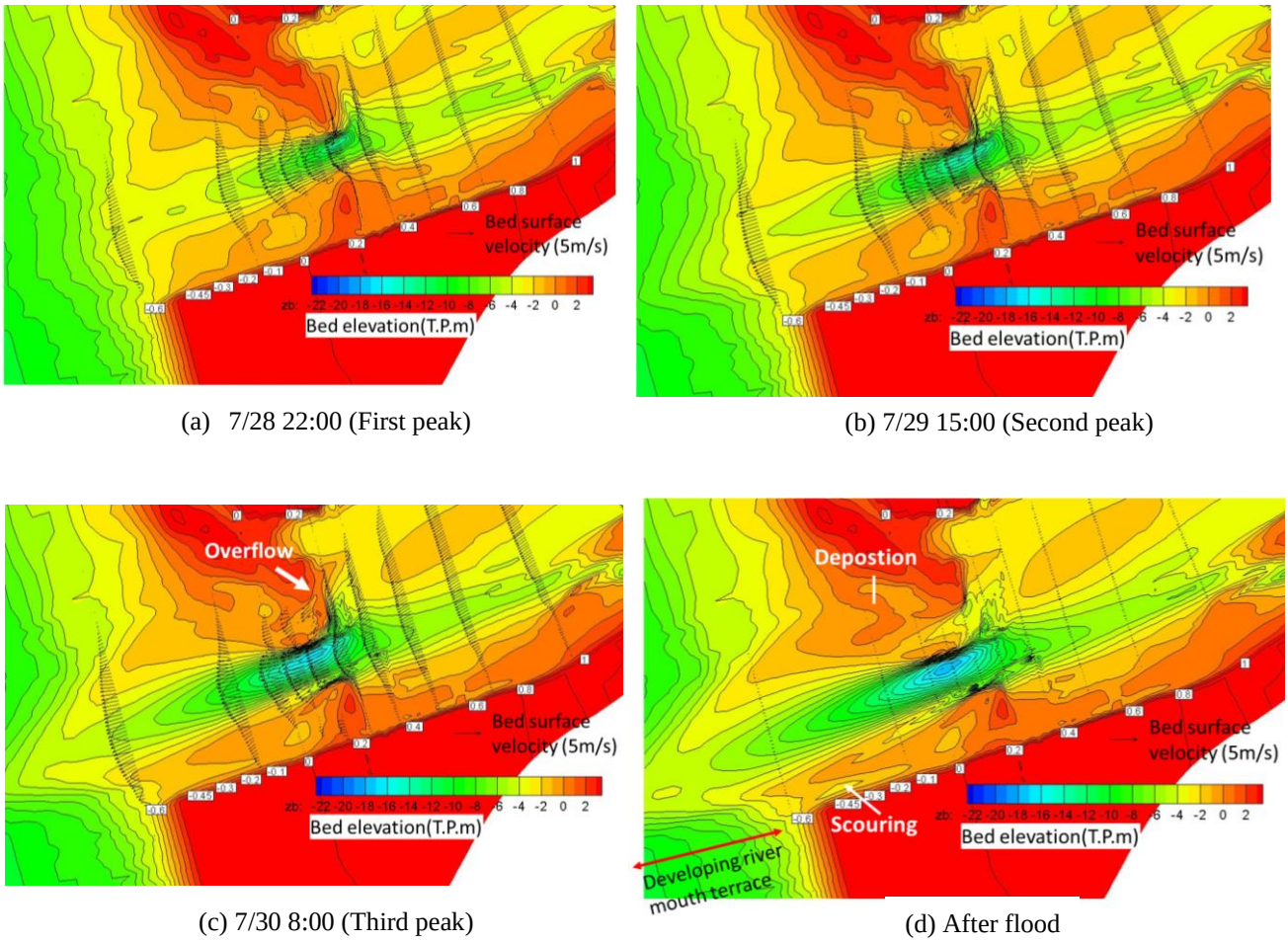

(a) 7/28 22:00 (First peak) (b) 7/29 15:00 (Second peak)

(c) 7/30 8:00 (Third peak) (d) After flood

Figure 9. the contours of calculated river bed topography around the river mouth sandbar during the flood.

4. CALCULATION RESULTS

Figure 5 indicates the comparison between observed and calculated discharge hydrographs in the Yokogoshi observation station at 13.5km point. And Figure 6 shows the comparison between the observed and calculated water surface profiles in the flood rising period. In 2011 flood, the discharge hydrograph had three peaks shown in Figure 5. The first peak occurred on July 28th at 22:00, the second peak occurred on 29th at 15:00 and the third peak occurred on 30th 8:00. The calculation results could almost reproduce the time series of observed water surface profiles around those peak periods and the observed discharge hydrograph.

Figure 7 indicates the observed and calculated water level hydrographs at 0. 2km and 0.4km points where the water levels tended to be raised by the existing river mouth sandbar, respectively. The calculation results almost

explained the observed water level hydrographs around the times of each peak discharge, although the reproducibility of those during the low water levels was slightly low.

Figure 8 shows the observed cross-sectional bed profiles of sandbars before and after the flood and temporal changes in the calculated cross-sectional bed profiles on the river mouth (0.2km point) and the downstream of the sandbar (-0.45km point). And Figure 9 indicates the contours of time series of the calculated bed topography around the river mouth sandbar during the flood. The calculation results clarified that the flood flows overflowed the river mouth sandbar around the time of the third peak (7/30 8:00). After the third peak, it was found that the cross-sectional bed profile of the river mouth sandbar at 0.2km point was greatly scoured due to the overflows. The scoured sediments on the sandbar were transported and deposited longitudinally in the downstream of the sandbar (see Figure 9(d)). And those sediment depositions caused to slightly shift the directions of the main flows toward the left bank. Thus the river bed near the left bank around -0.45km point tended to be scoured.

Figure 10 indicates the longitudinal distributions of the amount of the calculated bed load and suspended load at 7/29 15:00 (the second peak) and 7/30 8:00 (the third peak discharge), respectively. The calculation results revealed that most of the sediments were transported in states of suspensions around the river mouth of the Aganogawa River. Figure 11 shows the differences between sediment entrainments from bed load motions to suspensions and the sedimentations from suspensions to bed load motions at the time of the third peak. The Red color means suspended sediment entrainments from bedload and the blue color means sedimentation from suspension to bedload. The large amount of sediment entrainments from bed load motions to suspensions occurred on the sandbar of river mouth around 0.2km point. Therefore the amount of suspended load increased longitudinally due to the increasing transitions from bed load motions on the river mouth sandbar around 0.2km as shown in Figure 10, while the amount of bed load decreased longitudinally around there. These calculation results demonstrated the interactions between bed load motions and suspensions were calculated properly in the developed calculation method.

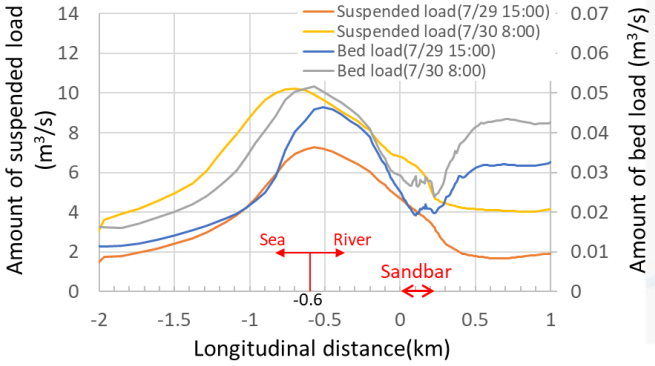

Figure 10. Longitudinal distributions of amount of the calculated bed load and suspended load at 7/29 15:00 (Second peak) and 7/30 8:00 (Third peak discharge).

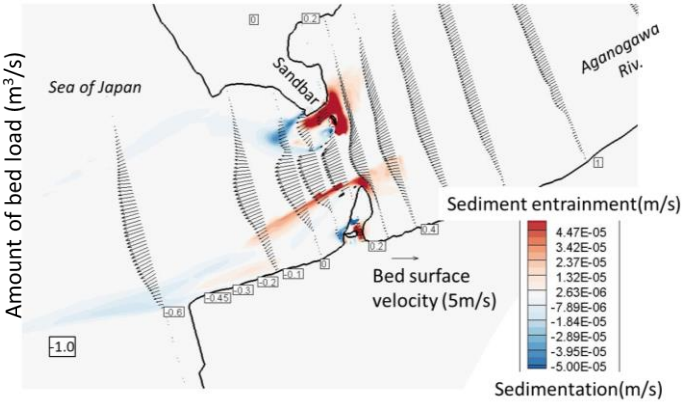

Figure 11. Differences between sediment entrainments from bed load motions to suspensions and the sedimentations from suspensions to bed load motions.

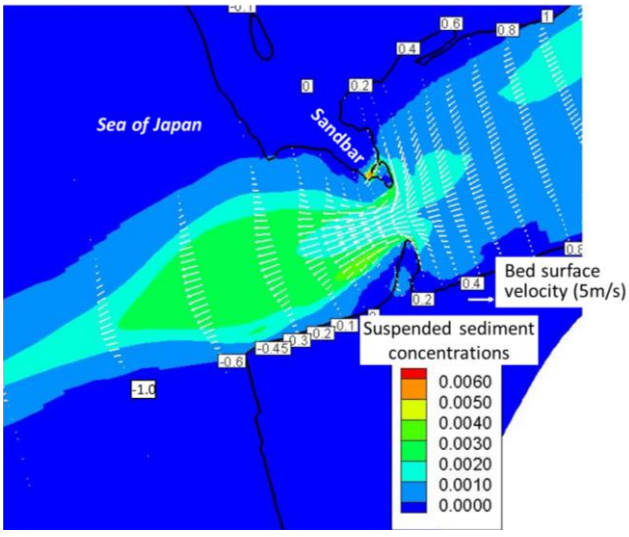

(a) 7/29 15:00 (Second peak)

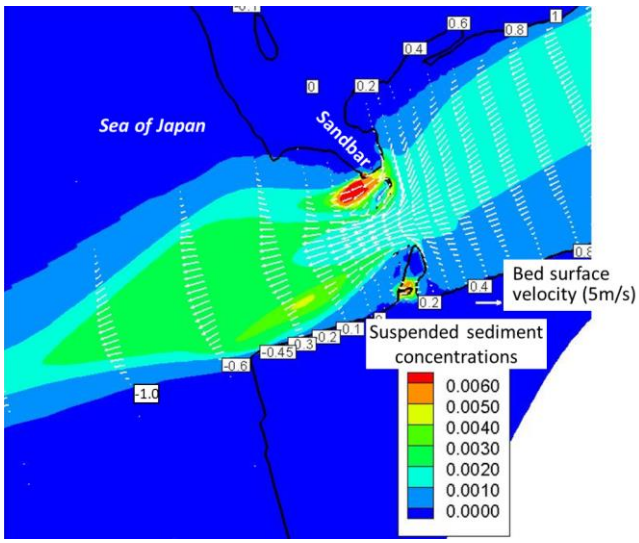

(b) 7/30 8:00 (Third peak)

Figure 12. the contours of suspended sediment concentrations near the beds around the river mouth sandbar at 7/29 15:00 (Second peak) and 7/30 8:00 (Third peak discharge).

Figure 12 shows the contours of the suspended sediment concentrations near the beds around the river mouth sandbar at 7/29 15:00 (the second peak) and 7/30 8:00 (the third peak discharge). The high concentrations of suspended sediments occurred on the river mouth sandbar due to the strong sediment entrainments by the overflows. And those high concentrations and the amount of suspended load shown in Figure 10 were gradually decreasing due to the sedimentations for the longitudinal direction toward sea. The sedimentations induced the developments of the river mouth delta as shown in Figure 9(d).

5. CONCLUSIONS

The quasi-three dimensional flow and bed variation analysis method was constructed by considering non-equilibrium motions and interactions between bed load motions and suspensions of sediments and the changes in the river mouth sandbar in the Aganogawa River was investigated by this method.

The developed flood flow and bed variation analysis method elucidated processes of the opening widths enlargements in the river mouth sandbar and developments of the river mouth terrace by sediment depositions in the sea due to the 2011 flood. The calculation results indicated that the large amount of sediments were transported in states of suspensions and the transitions from bed load motions to suspensions largely occurred on the river mouth sandbar due to the overflow.

REFERENCES

Bose SK, Dey S (2013). Sediment entrainment probability and threshold of sediment suspension: exponential-based approach. *Journal of Hydraulic Engineering*, ASCE, Vol.139(10), pp.1099–1106.

Chauchat, J., Cheng, Z., Nagel, T., Bonamy, C. and Hsu, T.J. (2017). SedFoam-2.0: a 3-D Two-Phase Flow Numerical Model for Sediment Transport. *Geoscientific Model Development*, Vol.10, Issue12, pp.4367–4392.

Itakura, T. and Kishi, T. (1980). Open Channel Flow with Suspended Sediments. *Journal of the Hydraulic Division*, ASCE, HY8, 1325-1343.

Leo C. van Rijn. (1984). Sediment Transport, Part I: Bed Load Transport. *Journal of Hydraulic Engineering*, Vol.110, Issue10, pp.1431-1456.

Nakagawa, H., Tsujimoto, T., Murakami, S. and Gotoh, H. (1990). Transition Mechanism from Saltation to Suspension in Bed-Material-Load Transport. *Journal of hydroscience and hydraulic engineering*, Vol.8(1), pp.41-54.

Osada, K., Fukuoka, S. and Ohgushi, H. (2013). Study of flood flow and gravel river bed variation analysis in the Satsunai River. Advances in River Sediment Research, *Proceedings of 12th International Symposium on River Sedimentation*, ISRS, pp.589-598.

Ota, K., Sato, T. and Nakagawa, H. (2015). 3d numerical model of sediment transport considering transition from bed-load motion to suspension - application to a scour upstream of a cross-river structure -. J*ournal of Japan Society of Civil Engineers, Ser. B1 (Hydraulic Engineering)*, Vol.71, Issue4, pp.I_883-I_888.

Takemura, Y. and Fukuoka, S. (2019). Analysis of flows in undular and breaking hydraulic jumps by non-hydrostatic quasi three-dimensional model considering flow equations on boundary surfaces (Q3D-FEBS). 36th IAHR World Congress, pp.2049-2055.

Tateyama, M., Fukuoka, S. and Ishikawa, T. (2018). Study on flushing mechanism of river mouth sandbar due to large flood. *Journal of Japan Society of Civil Engineers, Ser. B1 (Hydraulic Engineering)*, Vol.74, Issue 4, pp.I_715-I_720.

Zyserman, J. A., and Fredsøe, J. (1990). Data analysis of bed concentration of suspended sediment. *Journal of Hydraulic Engineering*, ASCE, 120(9), pp.1021–1042.